Metal–single-molecule–semiconductor junctions formed by a radical reaction bridging gold and silicon electrodes

*Chandramalika R. Peiris[1], Yan B. Vogel[1], Anton P. Le Brun[2], Albert C. Aragonès[3], Michelle L. Coote[4], Ismael Díez-Pérez [3], Simone Ciampi[*1] and Nadim Darwish[*1]*

[1]School of Molecular and Life Sciences, Curtin Institute of Functional molecules and Interfaces, Curtin University, Bentley, WA 6102, Australia

[2]Australian Centre for Neutron Scattering, Australian Nuclear Science and Technology Organization (ANSTO), Lucas Heights, NSW 2234, Australia.

[3] Department of Chemistry, Faculty of Natural & Mathematical Sciences, King's College London, Britannia House, 7 Trinity Street, London SE1 1DB, United Kingdom.

[4] ARC Centre of Excellence for Electromaterials Science, Research School of Chemistry, Australian National University, Canberra, Australian Capital Territory 2601, Australia

Email: nadim.darwish@curtin.edu.au;simone.ciampi@curtin.edu.au

KEYWORDS: Electrochemically modified interfaces, surface chemistry, self-assembled monolayers (SAM), radical reaction, single-molecule electronics.

ABSTRACT: Here we report molecular films terminated with diazonium salts moieties at both ends which enables single-molecule contacts between gold and silicon electrodes at open circuit via a radical reaction. We show that the kinetics of film grafting is crystal-facet dependent, being more favourable on ⟨111⟩ than on ⟨100⟩, a finding that adds control over surface chemistry during the device fabrication. The impact of this spontaneous chemistry in single-molecule electronics is demonstrated using STM-break junction approaches by forming metal–single-molecule–semiconductor junctions between silicon and gold source and drain, electrodes. Au–C and Si–C molecule-electrode contacts result in single-molecule wires that are mechanically stable, with an average lifetime at room temperature of 1.1 s which is 30–400 % higher than that reported for conventional molecular junctions formed between gold electrodes using thiol and amine contact groups. The high stability enabled measuring current-voltage properties during the lifetime of the molecular junction. We show that current rectification, which is intrinsic to metal-semiconductor junctions, can be controlled when a single-molecule bridges the gap in the junction. The system changes from being a current-rectifier in the absence of molecular bridge to an ohmic contact when a single-molecule is covalently bonded to both silicon and gold electrodes. This study paves the way for the merging of the fields of single-molecule and silicon electronics.

1. INTRODUCTION

One of the main goals of molecular electronics is to use molecular films, or even single molecules, as functional electronic components such as diodes, resistors or transistors.[1-3] The biggest challenge preventing this concept from becoming reality is the lack of mechanically robust contacts of an organic molecule with source and drain electrodes.[4-5] To date, the most used electrode–molecule contacts have relied on the chemisorption of thiols on gold surfaces.[6-11] Such contacts are spontaneously formed from dilute solutions of thiols.[12-14] Although widely used, molecular electronics on gold platforms suffer from major drawbacks, such as the lability of the

S–Au bonds, electric field-induced structural changes and the lack of tunability of the electric properties of the gold substrate which limits the scope of these junctions.[15-16] In the last few years there has been an increasing interest in expanding the field of molecular electronics from gold towards semiconducting platforms, particularly GaAs[17-18] and Si.[19-21] It is anticipated that combining the vast and tunable range of the electrical properties of semiconductors with the chemical variety of molecules, new technological development can be achieved.

Among all the methods developed to modify semiconducting surfaces, the most common is the addition of an 1-alkene or 1-alkyne to a silicon radical to produce a covalent Si–C bond.[22-23] This process, although successful in forming well packed monolayers, requires either a source of UV-light or heat, as well as a concentrated solution of the alkene or alkyne molecule. Such assembly requirements are not viable to form a stable contact in molecular electronics devices, and it is therefore essential to find new chemical strategies to form contacts on silicon electrodes that are of comparable ease to those for standard thiol-based contacts on gold. In this context, the cathodic electrochemical reduction of aryldiazonium salts is one of the most widely used methods for chemically modifying metal, carbon and silicon surfaces, which leads to strong covalent bonds.[21, 23-33] Tao and co-workers[34] have reported the formation of single-molecule junctions in the presence of diazonium molecules in solution by means of electrochemically reducing, simultaneously, the two diazonium terminal groups. This allowed to form two Au–C covalent bonds, *in-situ,* using a bipotentiostatic "gated" control of two gold electrodes against a reference electrode. The Au–C contact is significantly more stable to what is achievable with thiol and amine molecules, which are typically used for molecular junction contacts.

In this study the diazonium radical reaction is demonstrated on semi-conducting electrodes, Si ⟨111⟩ and Si ⟨100⟩, and is utilized to form metal–molecule–semiconductor junctions at the single-

molecule level. We use two axial diazonium terminal groups to form covalently bonded molecular junctions on gold and silicon electrodes. We show that molecular contacts on both silicon and gold can be made spontaneously by using a diazonium salt of high redox potential such that it can be reduced and consequently bridge both electrodes at open circuit. The role of surface energy was investigated by studying the effect of crystal orientation (⟨100⟩ *vs* ⟨111⟩) on the grafting process. Our findings remove the need of applying an electrochemical gate because the top and bottom contacts can be formed on the same molecule spontaneously and yet sequentially. Further our strategy does not require the continuous presence of molecules in the solution, which simplifies device fabrication for molecular junctions. The molecular films reported here are characterized by electrochemical methods, X-ray reflectometry and by atomic force microscopy. The scope of this chemistry in single-molecule electronics is demonstrated by means of single-molecule STM-break junction technique to electrically bridge silicon and gold electrodes via axial diazonium terminal groups. The mechanical stability of these covalently bonded single-molecule junctions were investigated using the "blinking approach" and compared to standard Au–molecule contacts. Current-voltage properties are reported for junctions made in the presence or absence of molecules; demonstrating the tunability of semiconductor junctions by the electronics of a single-molecule.

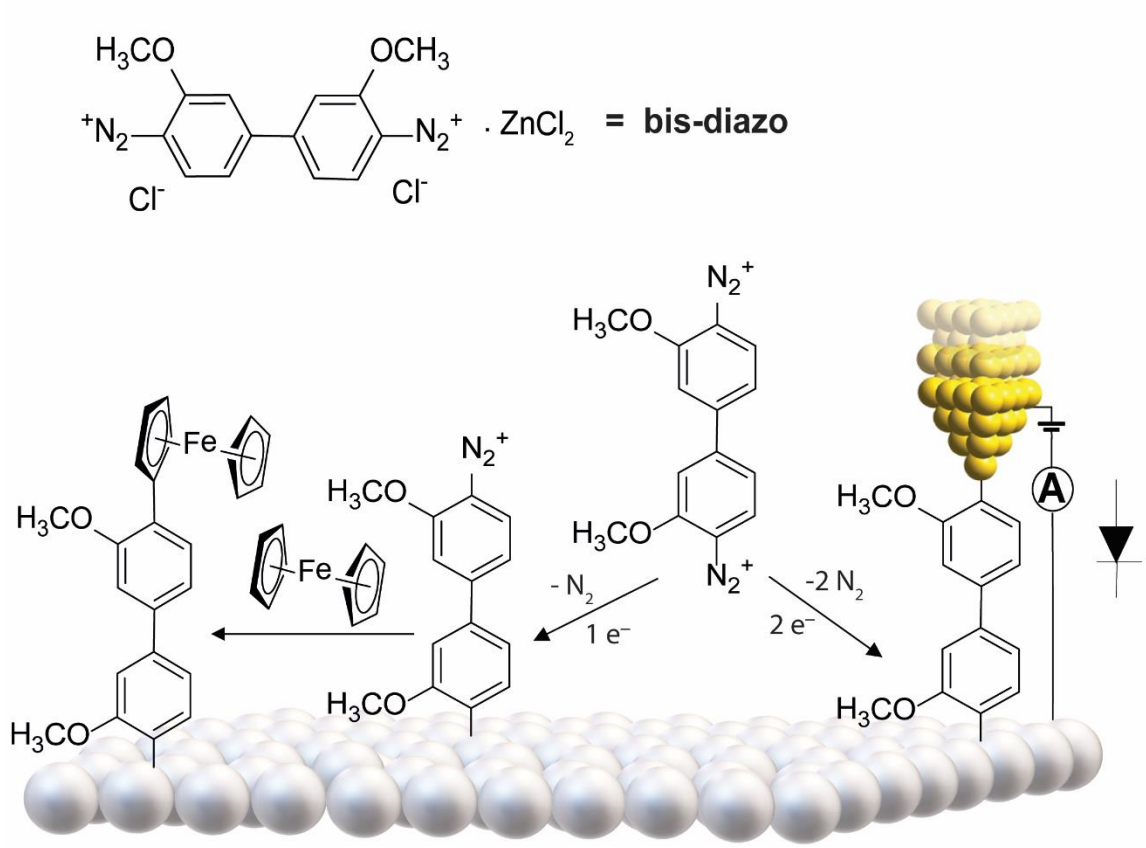

Figure 1. Structure of the molecule (**bis-diazo**) studied and a schematic describing its reaction with surface and tip electrodes or with ferrocene. The surface and tip electrodes can be gold or silicon.

2. RESULTS AND DISCUSSION

2.1. Electro- versus spontaneous-grafting of bis-diazo on gold

Multiple reduction peaks during the electrografting of diazonium salts on polycrystalline Au have been reported for several molecules and are often attributed to a range of different phenomena. One hypothesis is that multiple waves originates from the presence of different crystallographic facets present on the polycrystalline Au surface.[35-38] To test this hypothesis we deliberately varied the crystallinity of the Au surface from a completely polycrystalline sample to a single crystal ⟨111⟩ surface (Figure 2a−c). The degree of crystallinity was estimated from the gold oxide anodic wave in cyclic voltammetry: a single oxidation peak indicates that the surface is 100% ⟨111⟩ while multiple or broad oxidation waves are ascribed to a polycrystalline sample (Figure 2a-c). For the

reduction of **bis-diazo** on highly oriented single crystal Au⟨111⟩, only a single wave is observed at −70 mV (Figure 2d). A second wave at more negative potentials (−350 mV) appears for the reduction of **bis-diazo** on other Au crystal orientations. For instance, the reduction of **bis-diazo** on a 70% Au⟨111⟩ surface (Figure 2e) results in two waves, with that assigned to ⟨111⟩ being almost three folds larger than that centered at −350 mV (Figure 2e). Completely polycrystalline samples (Figure 2f) shows multiple broad waves between 0 and −400 mV, again highlighting the correlation between the crystallinity of the surface and the shifts in biases required to graft **bis-diazo**.

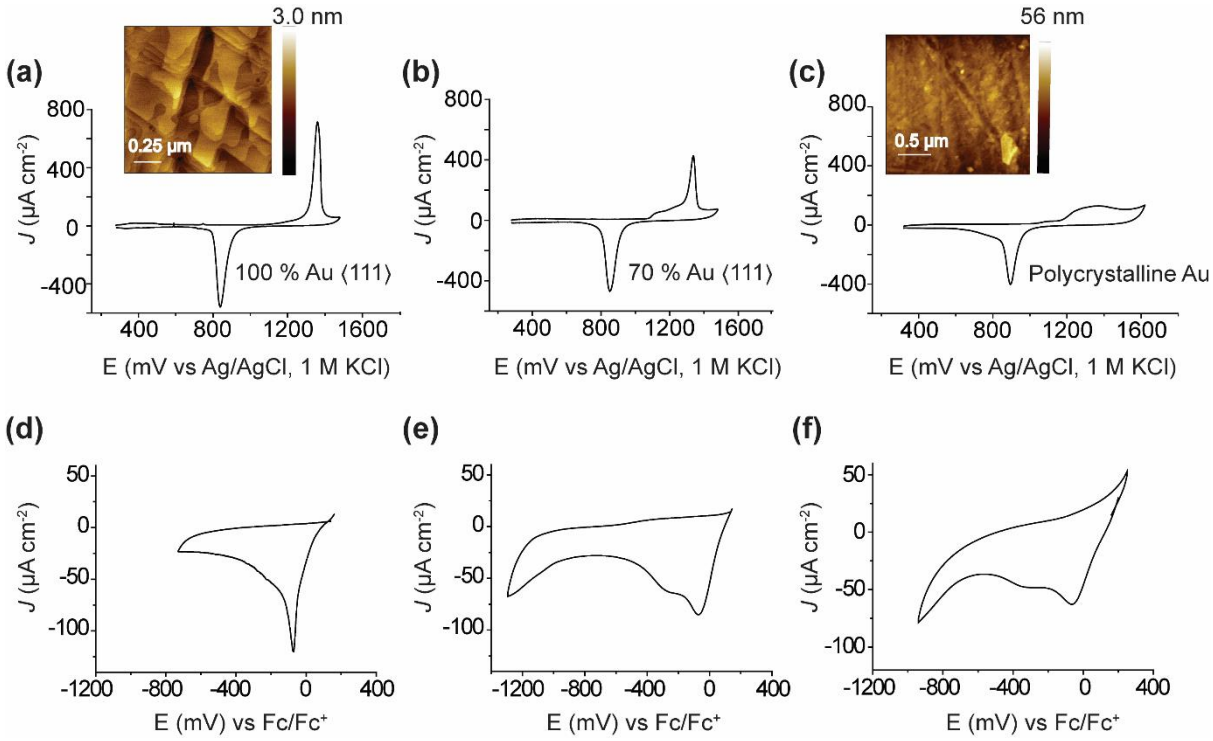

Figure 2. Electrochemical grafting of **bis-diazo** on mono- and poly-crystalline gold surfaces. Cyclic voltammograms showing the oxidation and reduction waves of a) 100 % single crystal Au ⟨111⟩. The Inset in (a) shows an AFM topography image of the single crystal surface. b) 70% Au ⟨111⟩ and c) polycrystalline gold (0.5 M H_2SO_4 as the electrolyte) at scan rate 100 mV s^{-1}. The potential is expressed in mV against aq. Ag/AgCl electrode (1 M KCl). The inset in (c) shows an AFM topography image of the polycrystalline Au surface. The gold oxidation wave is a single peak at around +1300 mV for 100% Au ⟨111⟩. (b–c) Multiple oxidation waves between +1000 mV and +1400 mV appear for 70% Au ⟨111⟩/30% polycrystalline in (b) and for a 100% polycrystalline surfaces in (c). (d–f) Electrochemical reduction waves for the grafting of **bis-diazo** (1 mM) with Bu_4NPF_6 (0.1 M) in a 1:49 (v/v) dimethyl sulfoxide/acetonitrile (DMSO/ACN) solvent mixture on the different gold surfaces shown in panels a–c. The scan rates in panels d–f are 50 mV s^{-1} and the potential is expressed in mV against Fc/Fc^+ (1 mM in ACN). The more polycrystalline the Au surface is the broader and the more split are the reduction waves.

The reduction potential of **bis-diazo** on Au⟨111⟩ is relatively anodic (−70 mV *vs* Fc/Fc^+, Figure 2), meaning the grafting could spontaneously occur even at open circuit. Following the reduction step, a radical intermediate will form a covalent bond between the organic molecule and the gold surface,[39-40] as schematized in Figure 3a. The surface-tethered molecule would still have a diazo group at the distal end, and this hypothesis was tested by resting a clean Au⟨111⟩ sample at open circuit in a solution of **bis-diazo** for 2 h, after which the sample was transferred to a ferrocene solution. Ferrocene can act as sacrificial electron donor, reducing the diazonium to generate a radical[39-40] that can in turn react with excess ferrocene in solution forming a covalent bond (see Figure 3a). The coupling reaction between the metallocene and the unreacted azo distal end of the monolayer formed at open circuit was then tested by means of measuring cyclic voltammograms. Cyclic voltammetry data for these films is shown in Figure 3c, and the amount of ferrocene units tethered on the surface are comparable to films formed by either spontaneous or potentiostatic electrolysis 2.30 (± 0.40) $\times 10^{-10}$ mol cm^{-2} equivalent to a 1.38 (± 0.24) $\times 10^{14}$ molecule cm^{-2} for the electrochemical grafting (Figure 3b) and 1.80 (± 0.29) $\times 10^{-10}$ mol cm^{-2} equivalent to 1.08 (± 0.17) $\times 10^{14}$ molecule cm^{-2} for the spontaneous process (Figure 3c).

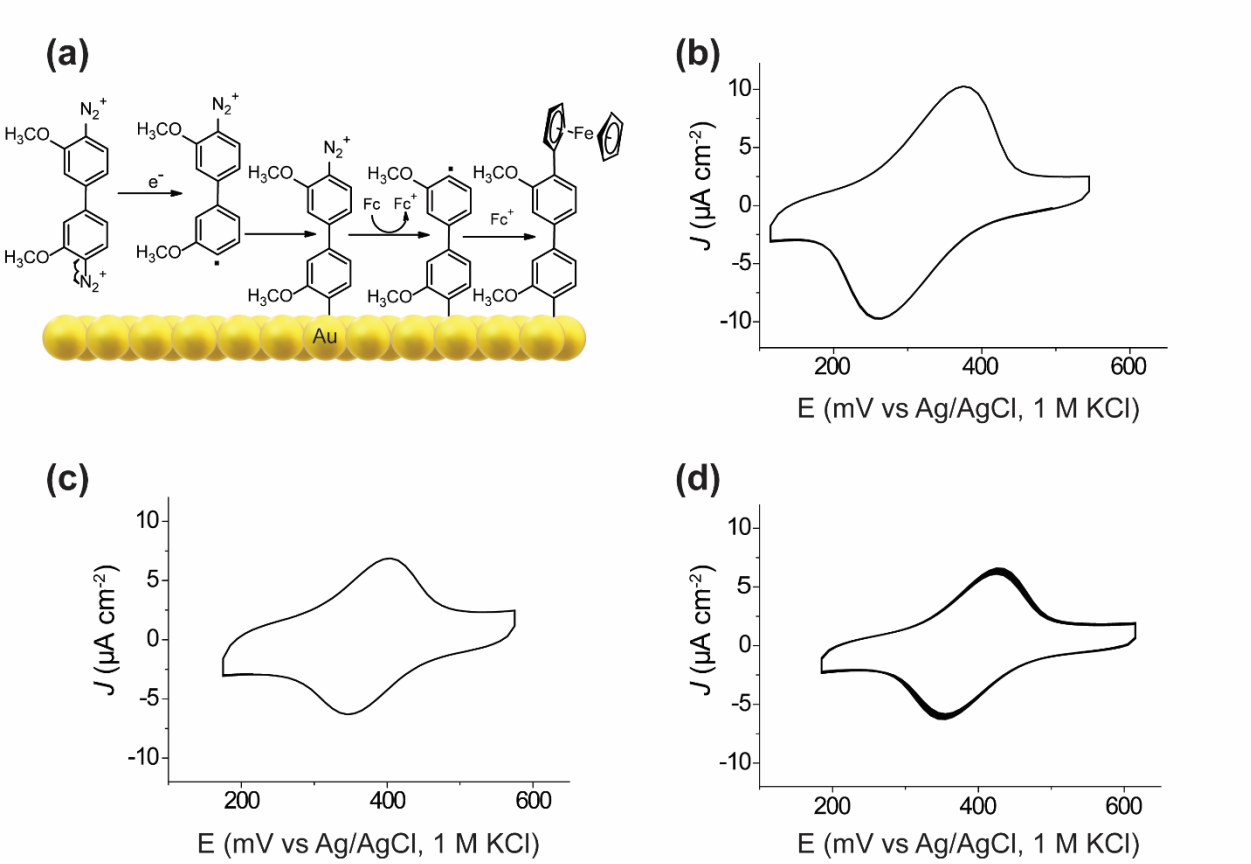

Figure 3. Electrochemical and spontaneous grafting of **bis-diazo** on Au⟨111⟩ followed by a reaction with ferrocene. a) Schematics describing the formation of a diazonium film on an Au surface and the reduction of the distal diazonium moiety by ferrocene molecules. b) Cyclic voltammogram for an Au⟨111⟩ surface that was first modified with **bis-diazo** then exposed to a solution of ferrocene. The electrochemical reduction was first performed via 1 potential cycle (0 to −1 V vs Fc/Fc^+) in a solution of **bis-diazo** (1mM) with Bu_4NPF_6 (0.1 M) in a 1:49 (v/v) DMSO/ACN solvent mixture. The surface was then exposed to a solution of ferrocene (1 mM in ACN) for 30 min at open circuit. Note that the schematic in (a) does not take into account the polymerization of the film, see Supporting Information, Figure S1 for details. c) Cyclic voltammogram for the spontaneous reduction of **bis-diazo,** by means of resting an Au⟨111⟩ sample in a solution of **bis-diazo** for 2 h at open circuit, followed by the spontaneous reaction with ferrocene (30 min) to indirectly probe the presence of an intact unreacted diazo group at the distal end of the monolayer. The potential scan rate is 50 mVs^{-1}. d) Stability of the interface tested by means of 30 repetitive cyclic voltammograms scans for a surface that is prepared in a similar way to that described in (c), see Figure S2, Supporting Information for details. The voltammograms in (b–d) were recorded in 1 M $HClO_4$ and the potential is expressed in mV against Ag/AgCl electrode (1 M KCl).

2.2. Electro- versus spontaneous-grafting of bis-diazo on silicon

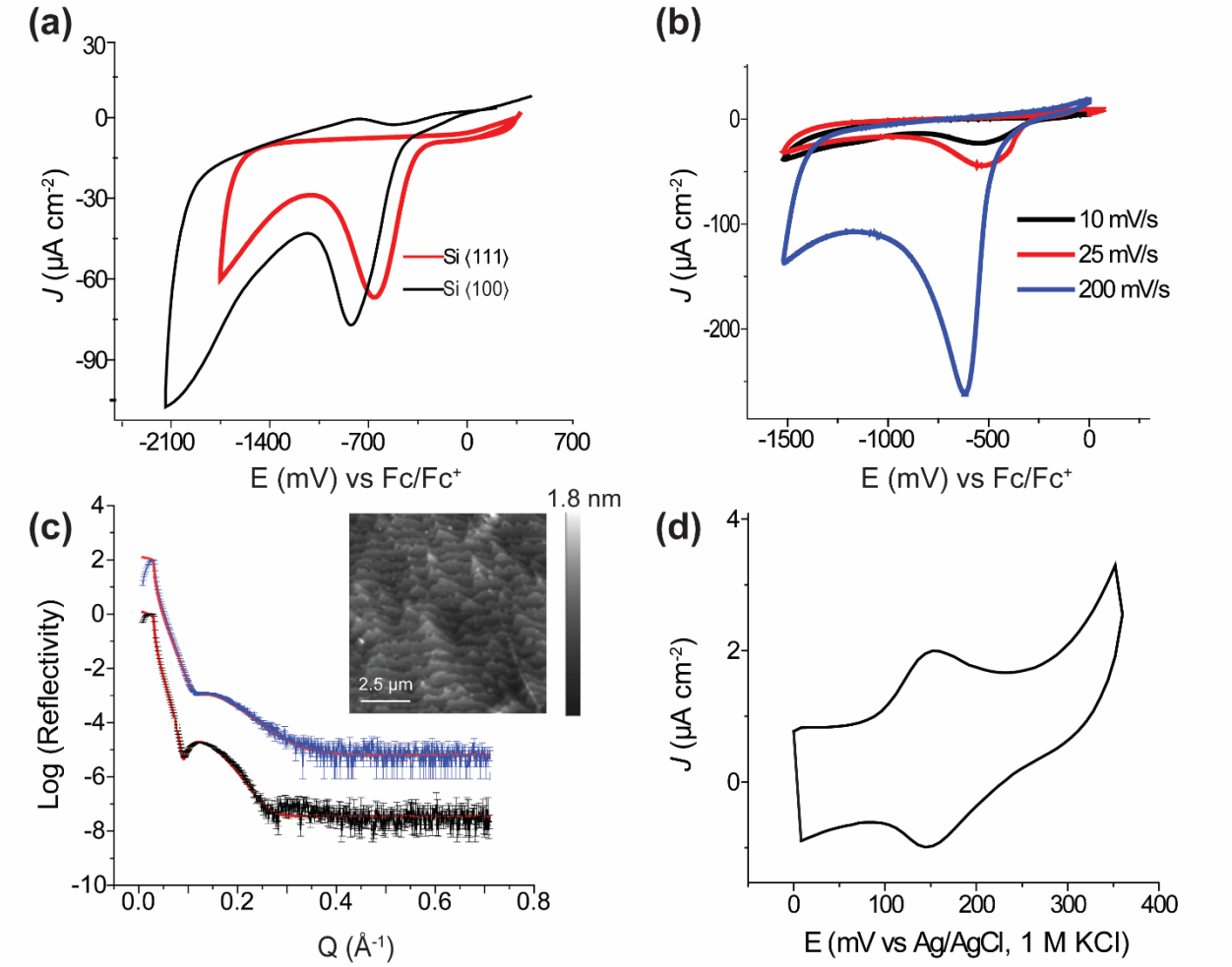

Figure 4. Electrochemical and spontaneous grafting of **bis-diazo** on silicon. a) Reductive grafting of **bis-diazo** (1 mM **bis-diazo** with 0.1 M Bu_4NPF_6 in a 1:49 (v/v) DMSO/ACN solvent mixture) on Si⟨111⟩ (red line) and on Si⟨100⟩ (black line) using one potential cycle (+0.4 V to −1.8 V for Si ⟨111⟩ and +0.5 V to −2.1 V for Si ⟨100⟩) at scan rate of 50 mV s^{-1}. The second potential cycle is shown in Figure S3, Supporting Information. b) Reduction of **bis-diazo** on Si⟨111⟩ using one potential cycle at different scan rates (10, 25 and 200 mV s^{-1}). c) XRR profiles for samples prepared by grafting **bis-diazo** on Si⟨111⟩–H electrochemically (black trace) or spontaneously (blue trace). The inset in (c) shows an AFM topography image of the Si⟨111⟩–H surface. The symbols with error bars are the collected data and the red solid lines are the fits to each data set. The data is vertically offset for clarity and the parameters used in the interpretation of the XRR data are listed in Table S1 of the Supporting Information. d) Cyclic voltammogram at a scan rate of 200 mV s^{-1} of a film of **bis-diazo** spontaneously prepared by resting a hydrogen-terminated Si⟨111⟩–H surface in a solution of **bis-diazo** for 8 h and then exposing it to a solution of ferrocene for 30 min. The potential in (a–b) is expressed in mV against Fc/Fc^+ (1 mM in ACN). The voltammogram in (d) was recorded in 1M $HClO_4$ and the potential is expressed in mV against Ag/AgCl electrode (1 M KCl).

Having established the formation of **bis-diazo** monolayers on gold surfaces, we then attempted to graft **bis-diazo** on silicon electrodes. Figure 4a shows that the wave for the electrochemical reduction of **bis-diazo** is centered at −650 mV and −830 mV on Si⟨111⟩ and Si⟨100⟩, respectively.

The thickness of the films was determined using X-ray reflectometry (XRR) and was found to be 2.43 nm when one potential scan, between 0 and −1.8 V vs Fc/Fc+ with a scan rate of 50 mV s^{-1}, was applied. A thickness of 2.43 nm means that **bis-diazo** polymerizes and the film comprises about 3 repeated **bis-diazo** units (Figure S1 and Table S1, Supporting Information).

As shown in Figure 4b, the electrochemical reduction of **bis-diazo** is scan rate-dependent, and digital simulations of the experimental voltammetry were used to gain quantitative insights on the heterogeneous electrochemical rate constant, k_{et}, values for the electrochemical reaction on both gold and silicon electrodes (Figure S4−S6, Supporting Information). We assumed an EC_{irrev} mechanism (E is the homogeneous redox step, **bis-diazo**$^{+}$/**bis-diazo**; C_{irrev} is the chemical homogeneous nitrogen loss, **bis-diazo** → **bis-diazo**$^{\bullet}$ + N_2). The k_{et} best-fit values are 4.0×10^{-3}cm s^{-1} for Au⟨111⟩, 1.0×10^{-5} cm s^{-1} for Au⟨100⟩, 2.0×10^{-7} cm s^{-1} for Si⟨111⟩, and 5.0×10^{-9}cm s^{-1} for Si⟨100⟩. The electrochemical rate is significantly slower for silicon, and both for silicon and gold the k_{et} drops from ⟨111⟩ to ⟨100⟩ facets. Furthermore, it is apparent from the absence of a return wave that the reduced form of the diazonium salt expels nitrogen after its initial electrochemical reduction with a rather large chemical rate (best-fit k_f of 5.0×10^{3} s^{-1}). The sluggish reduction kinetics on silicon indicates that for films of **bis-diazo** to form spontaneously at open circuit on silicon may require more time than that on gold. This was confirmed by measuring the ferrocene surface coverage *vs* time on both gold and silicon electrodes (Figures S7–S10, Supporting Information). The ferrocene molecules coverage increase from 7.67 (± 1.15) × 10^{11} molecule cm^{-2} to 3.89 (± 0.58) × 10^{12} molecule cm^{-2} when the resting time of the Si–H surface in the solution of **bis-diazo** increased from 2 min to 8 h (Figure S8, Supporting Information). In contrast, on the gold electrode the reaction reached equilibrium after 2 h.

As in the case of gold, a surface comprising both Si⟨111⟩ and ⟨100⟩ facets should show two discrete waves. To verify this, we etched crystallographically oriented Si⟨111⟩ pyramids on a Si⟨100⟩ surface by anisotropic etching in KOH solutions.[41-43] KOH etching creates samples with both ⟨111⟩ and ⟨100⟩ that can be used to probe *in-situ* the crystal-facets dependency of the electrochemical reduction.

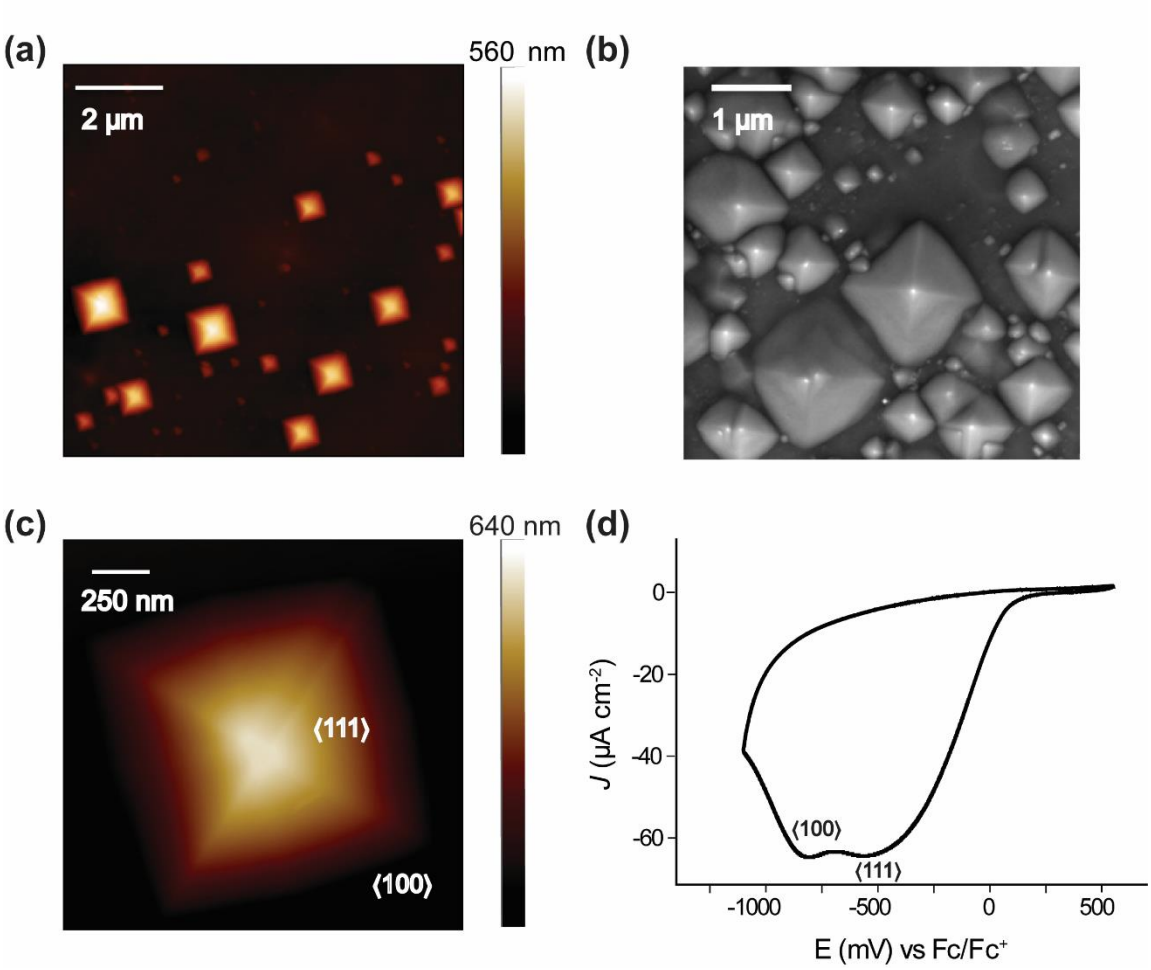

Figure 5. Electrochemical grafting of **bis-diazo** on crystalline silicon: Si⟨100⟩ vs Si⟨111⟩. a) AFM image of Si⟨111⟩ pyramids grown on Si⟨100⟩ by anisotropic etching of the surface in a solution of KOH solution. b) SEM image for the same surface. c) A zoom-in AFM image of a single pyramid. d) The electrochemical reduction wave of **bis-diazo** (1 mM **bis-diazo** with 0.1 M Bu_4NPF_6 in a 1:49 v/v DMSO/ACN mixture) on the sample presented in (a) and (b). The potential scan rate in (d) is 50 mV s^{-1} and the potential is expressed in mV against Fc/Fc^+ (1 mM in ACN).

The difference in the peak position for the reduction waves of **bis-diazo** on separate samples of Si⟨111⟩ and ⟨100⟩ is 180 mV, as in Figure 4a. Similar differences (ca. 200 mV) in the position of the reduction were observed for the mixed ⟨111/100⟩ (sample with pyramids; ⟨100⟩ surface etched

to expose ⟨111⟩ pyramids) (Figure 5b). The 200 mV difference is significant such that it can be used to control chemical reactivity on different silicon crystal orientation by controlling the applied reduction potential. The crystal-facet dependence is not restricted to the **bis-diazo** compound, and similar shifts in the diazo reduction wave were observed for 4-bromodiazonium salts electrochemically reduced on Si⟨111⟩, Si⟨100⟩ and on mixed ⟨111⟩/⟨100⟩ silicon surfaces (Figure S11, Supporting Information).

It is worth noting that since the source of electrons is not identified, the mechanism by which the spontaneous modification on both Au and Si occur is less clear than that when using the electrochemical method. The open circuit potential (OCP) measured for Au and Si electrode/electrolyte systems used in this study are −200 ± 100 mV and −300 mV ± 100 mV *vs* Fc/Fc^+, respectively. These values are relatively cathodic, and the formal potential of the **bis-diazo** is relatively anodic making it easily reducible to the aryl radical. The most plausible electron donors are the gold and silicon surfaces. Unlike bulk gold, which can usually be regarded as inert, surface defects, step edges and nanoscale protrusions are known to oxidize at significantly lower potentials. [44-45] Silicon oxidation can involve up to four electrons,[46] and the anodic growth of oxide can extend longitudinally away from the interface[47] meaning that the oxidation of limited surface areas can be sufficient to generate enough coulombs to reductively graft a **bis-diazo** monolayer. This scenario is in agreement with the slightly lower coverage measured by XRR (Table S1, Supporting Information) for the spontaneous versus electrochemical grafting. Another possibility or a contributor is the oxidation of adventitious impurities in the reaction solution; however this possibility is unlikely since the spontaneous reaction also occurred with an STM gold tip in a mesitylene solvent (section 2.3), a different environment to that used to form the **bis-diazo** films.

2.3. Single molecule STMBJ studies

The monolayer results of the previous section verify the spontaneous attachment of an electron-poor diazonium salt (**bis-diazo**) to both gold and silicon electrodes. The distal diazonium group of the molecule is conserved upon attachment, which opens the possibility for the further spontaneous attachment of a redox active organic molecule (e.g. ferrocene in Figure 3a), or more importantly, of a top metal point-contact to spontaneously close the electrical circuit. We proceeded to show this by forming Si−**bis-diazo**−Au junctions (Figure 6a). We performed single-molecule measurements using the scanning tunneling microscopy (STM) junction technique in the "blinking approach"[48-50] in which a gold STM tip is brought within tunneling distance to a silicon surface that was pre-modified with **bis-diazo** molecules. When a chemical bond is formed between the tip and the molecule a sudden current jump, or blink, appears in the current-time STM trace. A typical blink is shown in Figure 6b (inset) depicting the junction comprising a **bis-diazo** molecule passing a current of 3.5 ± 0.5 nA for 1.2 s. Figure 6b shows a histogram of the single-molecule conductance obtained from hundreds of blinks, with an average value of 90 ± 35 μG_0 (G_0,77.5 μS, is the conductance of a single quantum channel). The relative uniform conductivity distribution indicates that these molecular circuits are reproducible and of similar chemical nature. A histogram of blink lifetimes is shown in Figure 6b with the average being centered at 1.1 ± 0.2 s. This lifetime is significantly higher than previously reported for single-molecule junctions between gold surfaces using other chemistries.[51] As a comparison, the lifetime of an Au−**bis-diazo**−Au junction is 0.75 ± 0.15 s (Figure S12, Supporting Information) which is 30% less than that of the Au−**bis-diazo**−Si system. The difference was unexpected, given that the lifetime of both junctions should be limited by the relatively weak Au−molecule contact. We attribute the superior stability of the Au−**bis-diazo**−Si system to the presence of at least one robust point of contact (the silicon side), which can enhance the robustness of the junction if the mechanical pull is distributed more heavily on the

silicon side, which is a probable scenario as the STM tip is drifting away during measurements. The lifetime of the junctions was also compared on gold electrodes, but using a contact chemistry different than the Au−carbon of the Au−**bis-diazo**−Au junctions. The blinking lifetime for Au−molecule−Au system that relies on either Au−sulfur or Au–nitrogen contacts are 0.50 ± 0.10 s and 0.20 ± 0.05 s, respectively. These blinking lifetimes are several folds lower than that of the Au−**bis-diazo**−Au and Au−**bis-diazo**−Si contacts, highlighting the superior mechanical stability of the covalent Au−C and Si−C electrode contacts. (Figure S12, Supporting Information).

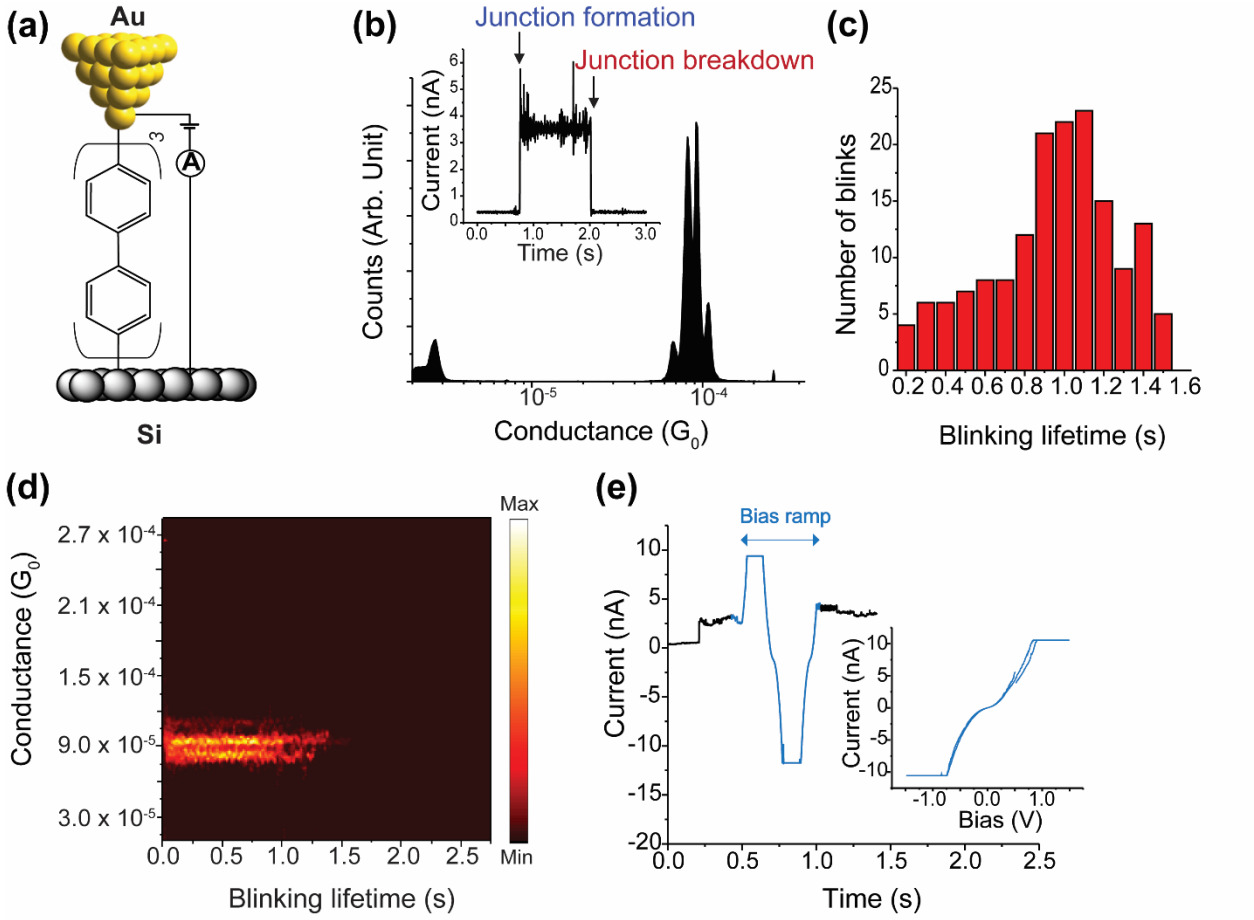

Figure 6. Single-molecule junction measurements of a Si⟨111⟩ surface pre-modified electrochemically (1 potential cycle from +0.4 V to −1.8 V Fc/Fc$^+$) by a **bis-diazo** film with a gold tip forming the top contact. a) Schematic depicting the molecular junction formed. b) Conductance histogram built from ca. 200 blinks averaging 90 ± 35 μG$_0$. The inset shows a representative Au–**bis-diazo**–Si blink, measured at a bias of 0.5 V. c) Histogram of blink lifetimes with the average being 1.1 ± 0.2 s d) Blinking color maps obtained by accumulating ca. 200 blinks and normalized to a common time origin. (e) Representative data for a voltage sweep applied during a blink of a single-molecule Au–**bis-diazo**–Si junction. The current is monitored before and after the voltage sweep to ensure the voltage is ramped while the molecular junction is still intact. The inset shows the corresponding current-voltage curve. The STM experiments were performed at room temperature in mesitylene.

The superior duration of the blinks formed by **bis-diazo** molecules is owed to its covalent bonding to both electrodes (Si−C and Au−C). Figure 6e shows that these junctions can be subjected to a voltage ramp of ± 1.5 V, for a duration of 0.5 s, without rupture. The timescale for the collection of current–voltage (I–V) is well within the ~1 s of the lifetime of a **bis-diazo** junction. I–V curves are symmetrical around the origin with very limited current rectification being observed. This is in contrast to the I–V curves measured on bare unmodified Si–H surfaces which showed current

rectification (Figure 7a). Even when the molecule is not bridging the two electrodes a shift towards a non-rectifying I-V curves are observed (Figure 7b).

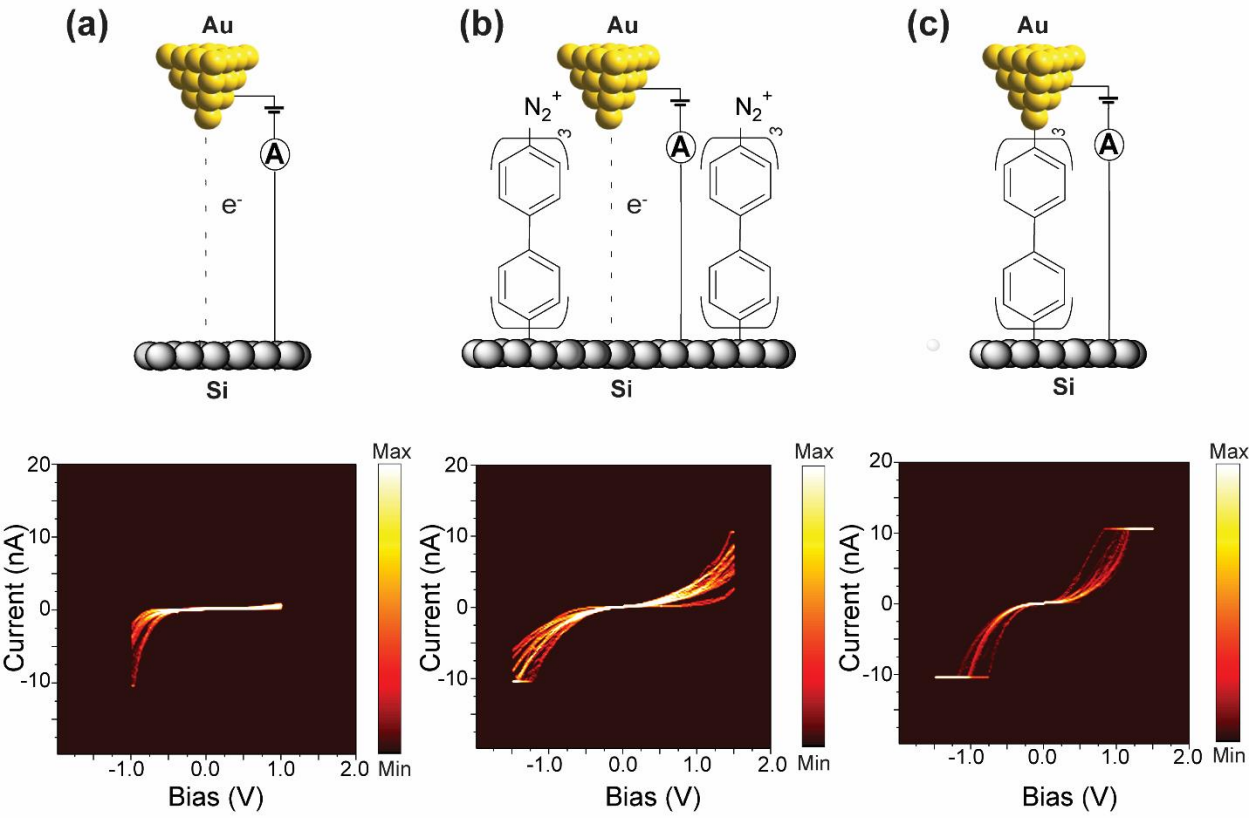

Figure 7. STM-current-voltage measurements. a) Schematic and current-voltage measurements of Au-Si tunneling junctions in the absence of **bis-diazo** molecules. b) Schematic and current-voltage measurements Au--**bis-diazo**--Si junctions in the absence of a "blink" and therefore absence of covalent bonding to both electrodes. c) Schematic and current-voltage measurements of Au–**bis-diazo**–Si junctions in which the **bis-diazo** molecule is covalently bonded to both electrodes. The data for each set is the accumulation of 30 different voltage sweeps and the bias is applied to the silicon surface. The characteristics of the current-voltage curves changes from rectifying in (a) to ohmic in the presence of a top contact with the molecule in (c) where the path of charge transfer is restricted to within the molecule. If the electrons can tunnel in the gaps between the molecules the rectification characteristic is intermediate. The STM experiments were performed at room temperature in mesitylene.

Of a particular note is the gradual decrease in the current rectification ratio (RR) when the system switches from a tunneling through space (Figure 7a, RR = 10–20 at ± 1V) to tunneling through the **bis-diazo** molecular film without a covalent attachment to the top gold electrode (therefore absence of a blink, Figure 7b, RR = 1–10 ± 1V), then to tunneling though the molecule when a blink forms (RR = 1–2 ± 1V). As a comparison we have performed I–V curves on symmetrical Au–**bis-diazo**–Au junctions (Figure S13, Supporting Information). Although the I–V of Au–**bis-**

diazo–Au junctions are also symmetrical, they are significantly different than the Au–**bis-diazo**–Si junctions. First, they are more conducting as evidenced by a larger I–V slope specifically in the small bias window of −0.5 to +0.5 V; and secondly there is no difference in the I–V curves shape nor in the non-rectifying properties of the junctions whether a molecule is connected between the gold electrodes or whether electrons are tunneling through space and not through a connecting **bis-diazo** molecule. This rules out the possibility of gold atom transferring to the silicon being the reason for the symmetric I–V curves for the Au–**bis-diazo**–Si junctions in Figure 7c. It also means that in Au–**bis-diazo**–Si junctions the covalently-connected molecule is providing a pathway for electrons to tunnel through the silicon's band gap. Non-rectifying junctions were recently observed for Au–molecule–GaAs junctions by Nichols and co-workers[17-18] in which the degree of rectification was found to depend on the molecules used to bridge the Au and the semiconducting GaAs electrodes: the more conjugated the molecules are (such as **bis-diazo**) the smaller the band gap and the more likely to have the lowest unoccupied molecular orbitals (LUMO) energy closer to the metal Fermi level enabling states for electron transport from the metal to the semiconductor under reverse bias. Another possible contributor to the high reverse bias current is the introduction of surface states that reduces the barrier height for electron transfer between the metal and the bottom of the conduction band.[52] This means that unlike conventional solid-state metal-semiconductor diodes, the metal**–bis-diazo–**semiconducting diodes can be tuned not only by the choice of the molecule but also by the nature of the top-contact (covalent versus non-contact).

3. CONCLUSION

We demonstrated that **bis-diazo** compounds form molecular films spontaneously, as well as electrochemically, on gold and silicon electrodes. The grafting is more sluggish on silicon that it is on gold and is crystal-facet dependent, being more favourable on ⟨111⟩ than it is on ⟨100⟩. This aspect of the work could become a way to address chemical reactivity at discrete locations, for

example by forming molecular monolayers on Si⟨111⟩ pyramids on a rather unmodified Si⟨100⟩ surface. This can be of significant practical implications in molecular electronics. We also show that the formed molecular films enable for the further attachment of top molecules and/or electrodes. We utilized this approach to form metal–molecule–semiconductor junctions between silicon and gold electrodes using the STMBJ technique. The single-molecule wires are mechanically stable, owed to the strong Au–C and Si–C contacts, with an average life time of 1.1 s, which is 30–400 % more stable than previous molecular junctions on gold electrodes and which enables current-voltage properties of the devices to be measured while the molecule is intact. We demonstrate that unlike conventional metal-semiconductor diodes, the metal–**bis-diazo**–semiconducting diodes can be tuned by a single-molecule contact and by the nature of the top-contact being covalent versus non-contact. This study offers a viable way to make top/bottom contacts between semiconductors and metals in miniaturized electronic devices and open prospects for a hybrid silicon and single-molecule electronics technology.

4. EXPERIMENTAL METHODS

4.1 Chemicals and Materials

Unless stated otherwise all chemicals were of analytical grade and used as received. Hydrogen peroxide (30 wt% in water), sulfuric acid (PuranalTM, 95–97%), ammonium fluoride (PuranalTM, 40 wt% in water), ammonium sulfite monohydrate (Sigma-Aldrich, $(NH_4)_2SO_3$, 92%) used for wafer cleaning plus etching, and silicon modification procedures were obtained from Sigma Aldrich. Acetonitrile (ACN) and dichloromethane (DCM) were distilled before use. *O*-Dianisidine bis(diazotized) zinc double salt (Sigma Aldrich, 98%), **bis-diazo** hereafter, 1,4-phenylenediamine (Sigma Aldrich ≥ 99%), benzene-1,4-dithiol (Sigma Aldrich, 99%), potassium hydroxide (VWR, 86%) and dimethyl sulfoxide (DMSO) were used as received. Tetrabutylammonium hexafluorophosphate (Bu_4NPF_6, Sigma-Aldrich, >99%), used as supporting electrolyte, was recrystallized twice from 2-propanol. Milli-Q^{TM} water (>18 MΩ cm) was used for surface cleaning

procedures and to prepare electrolytic solutions. Gold polycrystalline (rod like) electrodes were purchased from CH Instruments, USA. Gold single crystal electrodes (99.999%) were purchased from Goodfellow. Prime-grade, single-side polished silicon wafers were obtained from Siltronix, S.A.S. (Archamps, France) and were n-type (phosphorous doped), 500 ± 25 μm thick and either ⟨100⟩ ± 0.5° (with resistivity of 0.003 Ω cm), or ⟨111⟩ ± 0.5° (0.003 Ω cm).

4.2. Surface Modification

4.2.1. Polycrystalline Au modification

Au polycrystalline electrodes were polished to a mirror-like finish by means of mechanical polishing (ca. 5 min) on a micro cloth pad, using a slurry of 0.05 μm Al_2O_3. The electrodes were then rinsed with water, acetone, and then sonicated for 5 min in Milli-Q^{TM} water. The electrodes were then electrochemically cleaned by cycling them between −300 mV and +1600 mV (versus an aqueous Ag/AgCl reference electrode) in 0.5 M H_2SO_4. The electrode cleaning by cyclic voltammetry was continued until a reproducible voltammogram was obtained (typically after 25 cycles), and the electrode was then rinsed with Milli-Q^{TM} water and rested in distilled acetone prior to use.

4.2.2. Preparation of 100% Au⟨111⟩ and 70% Au⟨111⟩ single crystal

Single-crystal Au⟨111⟩ disks were cleaned in a hot Piranha solution for 2-3 min (3:1 (v/v) mixture of concentrated sulfuric acid to 30 wt % hydrogen peroxide), rinsed with Milli-Q^{TM} water and then annealed using a hydrogen flame. Annealed crystals were cooled down to room temperature, washed with Milli-Q^{TM} water, DCM and then blown dry under stream of argon gas. The crystals were then transferred to a deoxygenated solution of **bis-diazo** (1 mM) and Bu_4NPF_6 (0.1 M) in a 1:49 (v/v) mixture of DMSO and ACN and then either dynamically biased against a reference electrode or rested at open circuit.

For the preparation of surfaces exposing only ~70% of Au⟨111⟩, a single-crystal Au⟨111⟩ disk was melted on one of its edges (Figure S14, Supporting Information). The remaining intact surface area

of Au⟨111⟩ was estimated from the oxidation wave in cyclic voltammetry (Figure 2). The samples exposing ~70 % of Au⟨111⟩ were modified with **bis-diazo** in a similar way to that described for the 100 % Au⟨111⟩ crystals (section 4.2.2).

4.2.3. Si⟨111⟩ and Si⟨100⟩ modification

Silicon electrodes were cleaned and etched following literature procedures.[19] In brief, silicon wafers were cut into pieces (approximately 10 × 10 mm), cleaned for 30 min in hot Piranha solution, rinsed with Milli-Q^{TM} water and then etched with a deoxygenated 40 wt% aqueous ammonium fluoride solution for 13 min (Figure S15, Supporting Information). This process leads to a hydrogen-terminated silicon surface (Si–H). To the etching bath was added a small amount (ca. 5 mg) of ammonium sulfite. The etched samples were rinsed sequentially with Milli-Q^{TM} water, DCM and blown dry in a stream of argon before modifying the silicon surface using the same procedure as described in section 4.2.2.

4.2.4. Formation of ⟨111⟩ pyramids on silicon ⟨100⟩

Hydrogenated n-type silicon ⟨100⟩ substrates (generally 10 × 10 mm in size) were rinsed with DCM, 2-propanol and Milli-Q^{TM} water, and then dried under the steam of argon. The samples were then etched for 90 min in a 20 % (w/v) aqueous solution of potassium hydroxide (10 mL) with 2-propanol (200 μL) and kept at 45 °C. The etched samples were then rinsed with copious amounts of water before a final etching step in deoxygenated 40% aqueous ammonium fluoride solution (13 min) followed by modification with the **bis-diazo** film as described in section 4.2.2.

4.3. Electrochemical measurements

All electrochemical measurements were performed using a CHI650 (CH Instruments, USA) electrochemical workstation and a conventional three-electrode system with a platinum wire as the auxiliary electrode. An Ag/AgCl aqueous electrode (1.0 M KCl, CH Instruments, USA) served as the reference in the electrochemical cleaning of gold surfaces, while a non-aqueous “leakless”

Ag/AgCl electrode (eDAQ, part ET072-1) was used in the experiments for the **bis-diazo** reduction. The non-aqueous "leakless" reference electrode (3.4 M KCl) was calibrated before and after each experiment against the position, on an Au electrode, of the ferrocene/ferricenium couple Fc/Fc^+ (1 mM ferrocene solutions in acetonitrile containing 0.1 M Bu_4NPF_6). All potentials are reported versus the apparent formal potential of the Fc/Fc^+ couple unless otherwise specified.

4.4. Atomic Force Microscopy (AFM)

Atomic force microscopy images were obtained using Bruker dimension microscope operating in tapping mode. All images were obtained in air, at room temperature, and using silicon nitride cantilevers (TESPA from Bruker, with a spring constant of 20 N m^{-1}).

4.5. Scanning electron microscopy (SEM)

The SEM images were obtained using a Zeiss Neon 40EsB FESEM equipped with a Schottky field emission gun operating at 5 kV and a chamber pressure of 4×10^{-6} mbar and a Tescan Mira3 FESEM, also equipped with a Schottky field emission gun operating at 5 kV, and a chamber pressure of 3×10^{-2} Pa.

4.6. STM break junction

STM break junction (STMBJ) experiments were performed with a PicoSPM I microscope head controlled by a 'Picoscan 2500' controller, from Agilent. Data were acquired using a NI-DAQmx/BNC-2110 National Instruments data acquisition system and analysed with a code written with the LabVIEW software. Single-molecule conductivity measurements were performed using the STMBJ in the blinking approach under fixed electrodes gap separation in a solution of mesitylene. The tunnelling current is first stabilized then current transients are captured. When a molecule bridges both electrodes, a sudden jump and 'blink' in the captured current is obtained. Conductance histograms were built by the accumulation of hundreds of individual blinks. The blinking histograms give information about the average conductivity of the single-molecule

junctions that form spontaneously between the two electrodes, as well as information on their mechanical stability (blink lifetimes).

4.7. X-ray reflectometry (XRR)

Specular X-ray reflectometry was conducted as previously described[19, 22, 53] on a Panalytical Ltd X′Pert Pro instrument. The instrument has a rotating anode source (Cu Kα radiation, λ = 1.54 Å), has beam focusing using a Göbel mirror, and fixed collimation slits of 0.1 mm. Measurements were conducted at the solid-air interface under ambient conditions using angles of incidence from 0.05° to 5.00° in 0.01° steps for 20 seconds per step. The raw data was processed using in-house software so that the critical edge was normalised to a reflectivity of unity and the data was presented as reflectivity versus momentum transfer, Q, defined as:

$$Q = \frac{4\pi \sin\theta}{\lambda}$$

where λ is the X-ray wavelength and θ is the angle of incidence. Data analysis was conducted using the MOTOFIT software package, which utilises an Abele's matrix method and a least-squares regression of varying the fitted parameters until a best fit that matches the experimental data is achieved.[54] The organic material was fitted using a single layer defined by its thickness, roughness, and scattering length density (SLD), ρ, defined as:

$$\rho = \frac{r_e \sum Z_i}{V_m}$$

where V_m is the total molecular volume (determined to be 237 Å^3 for **bis-diazo**), Z_i is the atomic number of each atom in the species, and r_e is the Bohr electron radius (2.818 ×10^{-5} Å). The theoretical SLD (ρ_t) of **bis-diazo** was determined to be 16.69 ×10^{-6} Å^{-2}. The number of molecules per cm^2 was determined from the fitted values as follows:

$$molecules\ per\ cm^2 = \frac{\tau \rho_f 10^{16}}{V_m \rho_t}$$

Where τ is the fitted thickness and ρ_f is the fitted SLD.

ASSOCIATED CONTENT

Supporting Information

The Supporting Information is available free of charge on the ACS Publications website.

Digital simulation for the electrochemical measurements, additional electrochemical, AFM and STMBJ data (PDF).

AUTHOR INFORMATION

The authors declare no competing financial interest

Corresponding Authors

nadim.darwish@curtin.edu.au

simone.ciampi@curtin.edu.au

ACKNOWLEDGMENT

N.D. and S.C. thanks the Australian Research Council for DE160101101, DE160100732 and DP190100735 grants.

5. REFERENCES

(1) Ratner, M. A Brief History of Molecular Electronics. *Nat. Nanotechnol.* **2013,** *8* (6), 378-381.
(2) Tao, N. J. Electron Transport in Molecular Junctions. *Nat. Nanotechnol.* **2006,** *1* (3), 173-181.
(3) Xu, B.; Xiao, X.; Tao, N. J. Measurements of Single-Molecule Electromechanical Properties. *J. Am. Chem. Soc.* **2003,** *125* (52), 16164-16165.
(4) Zhang, Y.; Zhao, Z.; Fracasso, D.; Chiechi, R. C. Bottom-Up Molecular Tunneling Junctions Formed by Self-Assembly. *Isr. J. Chem.* **2014,** *54* (5-6), 513-533.
(5) Jia, C.; Guo, X. Molecule–Electrode Interfaces in Molecular Electronic Devices. *Chem. Soc. Rev.* **2013,** *42* (13), 5642-5660.
(6) Darwish, N.; Paddon-Row, M. N.; Gooding, J. J. Surface-Bound Norbornylogous Bridges as Molecular Rulers for Investigating Interfacial Electrochemistry and As Single Molecule Switches. *Acc. Chem. Res.* **2013,** *47* (2), 385-395.
(7) Darwish, N.; Eggers, P. K.; Ciampi, S.; Tong, Y.; Ye, S.; Paddon-Row, M. N.; Gooding, J. J. Probing the Effect of the Solution Environment Around Redox-Active Moieties Using Rigid Anthraquinone Terminated Molecular Rulers. *J. Am. Chem. Soc.* **2012,** *134* (44), 18401-18409.

(8) Rascón-Ramos, H.; Artés, J. M.; Li, Y.; Hihath, J. Binding Configurations and Intramolecular Strain in Single-Molecule Devices. *Nat. Mater.* **2015,** *14* (5), 517-522.
(9) Darwish, N.; Aragonès, A. C.; Darwish, T.; Ciampi, S.; Diez-Perez, I. Multi-Responsive Photo-and Chemo-Electrical Single-Molecule Switches. *Nano Lett.* **2014,** *14* (12), 7064-7070.
(10) Haiss, W.; Wang, C.; Grace, I.; Batsanov, A. S.; Schiffrin, D. J.; Higgins, S. J.; Bryce, M. R.; Lambert, C. J.; Nichols, R. J. Precision Control of Single-Molecule Electrical Junctions. *Nat. Mater.* **2006,** *5* (12), 995-1002.
(11) Wang, L.; Gong, Z. L.; Li, S. Y.; Hong, W.; Zhong, Y. W.; Wang, D.; Wan, L. J. Molecular Conductance through a Quadruple-Hydrogen-Bond-Bridged Supramolecular Junction. *Angew. Chem., Int. Ed.* **2016,** *55* (40), 12393-12397.
(12) Bensebaa, F.; Ellis, T. H.; Badia, A.; Lennox, R. Thermal Treatment of n-alkanethiolate Monolayers on Gold, as Observed by Infrared Spectroscopy. *Langmuir.* **1998,** *14* (9), 2361-2367.
(13) Huang, Z.; Chen, F.; Bennett, P. A.; Tao, N. Single Molecule Junctions Formed via Au−Thiol Contact: Stability and Breakdown Mechanism. *J. Am. Chem. Soc.* **2007,** *129* (43), 13225-13231.
(14) Huang, C.; Jevric, M.; Borges, A.; Olsen, S. T.; Hamill, J. M.; Zheng, J.-T.; Yang, Y.; Rudnev, A.; Baghernejad, M.; Broekmann, P. Single-Molecule Detection of Dihydroazulene Photo-Thermal Reaction using Break Junction Technique. *Nat. Commun.* **2017,** *8*, 15436.
(15) Darwish, N.; Eggers, P. K.; Ciampi, S.; Zhang, Y.; Tong, Y.; Ye, S.; Paddon-Row, M. N.; Gooding, J. J. Reversible Potential-Induced Structural Changes of Alkanethiol Monolayers on Gold Surfaces. *Electrochem. Commun.* **2011,** *13* (5), 387-390.
(16) McCreery, R. L.; Yan, H.; Bergren, A. J. A Critical Perspective on Molecular Electronic Junctions: There is Plenty of Room in the Middle. *Phys. Chem. Chem. Phys.* **2013,** *15* (4), 1065-1081.
(17) Vezzoli, A.; Brooke, R. J.; Ferri, N.; Higgins, S. J.; Schwarzacher, W.; Nichols, R. J. Single-Molecule Transport at a Rectifying GaAs Contact. *Nano Lett.* **2017,** *17* (2), 1109-1115.
(18) Vezzoli, A.; Brooke, R. J.; Ferri, N.; Brooke, C.; Higgins, S. J.; Schwarzacher, W.; Nichols, R. J. Charge Transport at a Molecular GaAs Nanoscale Junction. *Faraday Discuss.* **2018,** *210*, 397-408.
(19) Vogel, Y. B.; Zhang, L.; Darwish, N.; Gonçales, V. R.; Le Brun, A.; Gooding, J. J.; Molina, A.; Wallace, G. G.; Coote, M. L.; Gonzalez, J. Reproducible Flaws Unveil Electrostatic Aspects of Semiconductor Electrochemistry. *Nat. Commun.* **2017,** *8* (1), 2066.
(20) Aragonès, A. C.; Darwish, N.; Ciampi, S.; Sanz, F.; Gooding, J. J.; Díez-Pérez, I. Single-Molecule Electrical Contacts on Silicon Electrodes Under Ambient Conditions. *Nat. Commun.* **2017,** *8*, 15056.
(21) McCreery, R. L. Molecular Electronic Junctions. *Chem. Mater.* **2004,** *16* (23), 4477-4496.
(22) Zhang, L.; Vogel, Y. B.; Noble, B. B.; Goncales, V. R.; Darwish, N.; Brun, A. L.; Gooding, J. J.; Wallace, G. G.; Coote, M. L.; Ciampi, S. TEMPO Monolayers on Si (100) Electrodes: Electrostatic Effects by the Electrolyte and Semiconductor Space-Charge on the Electroactivity of a Persistent Radical. *J. Am. Chem. Soc.* **2016,** *138* (30), 9611-9619.
(23) Ciampi, S.; Harper, J. B.; Gooding, J. J. Wet Chemical Routes to the Assembly of Organic Monolayers on Silicon Surfaces via the Formation of Si–C Bonds: Surface Preparation, Passivation and Functionalization. *Chem. Soc. Rev.* **2010,** *39* (6), 2158-2183.
(24) Menanteau, T.; Dias, M. n.; Levillain, E.; Downard, A. J.; Breton, T., Electrografting via Diazonium Chemistry: the Key Role of the Aryl Substituent in the Layer Growth Mechanism. *J. Phys. Chem. C* **2016,** *120* (8), 4423-4429.
(25) Gooding, J. J. Advances in Interfacial Design for Electrochemical Biosensors and Sensors: Aryl Diazonium Salts for Modifying Carbon and Metal Electrodes. *Electroanalysis.* **2008,** *20* (6), 573-582.

(26) Combellas, C.; Kanoufi, F.; Pinson, J.; Podvorica, F. I. Sterically Hindered Diazonium Salts for the Grafting of a Monolayer on Metals. *J. Am. Chem. Soc.* **2008,** *130* (27), 8576-8577.
(27) Liu, G.; Liu, J.; Böcking, T.; Eggers, P. K.; Gooding, J. J. The Modification of Glassy Carbon and Gold Electrodes With Aryl Diazonium Salt: The Impact of the Electrode Materials on the Rate of Heterogeneous Electron Transfer. *Chem. Phys.* **2005,** *319* (1-3), 136-146.
(28) Mahouche-Chergui, S.; Gam-Derouich, S.; Mangeney, C.; Chehimi, M. M. Aryl Diazonium Salts: a New Class of Coupling Agents for Bonding Polymers, Biomacromolecules and Nanoparticles to Surfaces. *Chem. Soc. Rev.* **2011,** *40* (7), 4143-4166.
(29) Chen, P.; McCreery, R. L., Control of Electron Transfer Kinetics at Glassy Carbon Electrodes by Specific Surface Modification. *Anal. Chem.* **1996,** *68* (22), 3958-3965.
(30) Lehr, J.; Williamson, B. E.; Flavel, B. S.; Downard, A. J. Reaction of Gold Substrates with Diazonium Salts in Acidic Solution at Open-Circuit Potential. *Langmuir.* **2009,** *25* (23), 13503-13509.
(31) Brooksby, P. A.; Downard, A. J. Electrochemical and Atomic Force Microscopy Study of Carbon Surface Modification via Diazonium Reduction in Aqueous and Acetonitrile Solutions. *Langmuir.* **2004,** *20* (12), 5038-5045.
(32) Downard, A. J. Potential-Dependence of Self-Limited Films Formed by Reduction of Aryldiazonium Salts at Glassy Carbon Electrodes. *Langmuir.* **2000,** *16* (24), 9680-9682.
(33) Paulik, M. G.; Brooksby, P. A.; Abell, A. D.; Downard, A. J. Grafting Aryl Diazonium Cations to Polycrystalline Gold: Insights into Film Structure Using Gold Oxide Reduction, Redox Probe Electrochemistry, and Contact Angle Behavior. *J. Phys. Chem. C.* **2007,** *111* (21), 7808-7815.
(34) Hines, T.; Díez-Pérez, I.; Nakamura, H.; Shimazaki, T.; Asai, Y.; Tao, N. Controlling Formation of Single-Molecule Junctions by Electrochemical Reduction of Diazonium Terminal Groups. *J. Am. Chem. Soc.* **2013,** *135* (9), 3319-3322.
(35) Clavilier, J.; Armand, D.; Sun, S.; Petit, M. Electrochemical Adsorption Behaviour of Platinum Stepped Surfaces in Sulphuric Acid Solutions. *J. Electroanal. Chem.* **1986,** *205* (1-2), 267-277.
(36) Clavilier, J.; El Achi, K.; Rodes, A. In Situ Probing of Step and Terrace Sites on Pt (S)-[n (111)×(111)] Electrodes. *Chem. Phys.* **1990,** *141* (1), 1-14.
(37) Feliu, J.; Fernandez-Vega, A.; Aldaz, A.; Clavilier, J. New Observations of a Structure Sensitive Electrochemical Behaviour of Irreversibly Adsorbed Arsenic and Antimony From Acidic Solutions on Pt (111) and Pt (100) Orientations. *J. Electroanal. Chem. Interfacial Electrochem.* **1988,** *256* (1), 149-163.
(38) Benedetto, A.; Balog, M.; Viel, P.; Le Derf, F.; Sallé, M.; Palacin, S. Electro-Reduction of Diazonium Salts on Gold: Why Do we Observe Multi-Peaks? *Electrochim. Acta.* **2008,** *53* (24), 7117-7122.
(39) Beckwith, A.; Jackson, R.; Longmore, R. The Intermediacy of Free Aryl Radicals in the Reaction of O-Alkenyloxybenzenediazonium Salts with Ferrocene. *Aust. J. Chem.* **1992,** *45* (5), 857-863.
(40) Zou, C.; Wrighton, M. S. Synthesis of Octamethylferrocene Derivatives via Reaction of (Octamethylferrocenyl) Methyl Carbocation with Nucleophiles and Application to Functionalization of Surfaces. *J. Am. Chem. Soc.* **1990,** *112* (21), 7578-7584.
(41) Schröder, H.; Obermeier, E.; Steckenborn, A. Micropyramidal Hillocks on KOH Etched {100} Silicon Surfaces: Formation, Prevention and Removal. *J. Micromech. Microeng.* **1999,** *9* (2), 139-145.
(42) Palik, E.; Glembocki, O.; Heard Jr, I.; Burno, P.; Tenerz, L. Etching Roughness for (100) Silicon Surfaces in Aqueous KOH. *J. Appl. Phys.* **1991,** *70* (6), 3291-3300.

(43) Powell, O.; Harrison, H. B. Anisotropic Etching of {100} and {110}Planes in (100) Silicon. *J. Micromech. Microeng.* **2001,** *11* (3), 217-220.
(44) Masitas, R. A.; Zamborini, F. P. Oxidation of Highly Unstable <4 nm Diameter Gold Nanoparticles 850 mV Negative of the Bulk Oxidation Potential. *J. Am. Chem. Soc.* **2012,** *134* (11), 5014-5017.
(45) Rodríguez-López, J.; Alpuche-Avilés, M. A.; Bard, A. J. Interrogation of Surfaces for the Quantification of Adsorbed Species on Electrodes: Oxygen on Gold and Platinum in Neutral Media. *J. Am. Chem. Soc.* **2008,** *130* (50), 16985-16995.
(46) Nohira, T.; Yasuda, K.; Ito, Y. Pinpoint and Bulk Electrochemical Reduction of Insulating Silicon Dioxide to Silicon. *Nat. Mater.* **2003,** *2* (6), 397-401.
(47) Kinser, C. R.; Schmitz, M. J.; Hersam, M. C. Conductive Atomic Force Microscope Nanopatterning of Hydrogen-Passivated Silicon in Inert Organic Solvents. *Nano Lett.* **2005,** *5* (1), 91-95.
(48) Nichols, R. J.; Higgins, S. J. Molecular Junctions: Single-Molecule Contacts Exposed. *Nat. Mater.* **2015,** *14* (5), 465-466.
(49) Nichols, R. J.; Haiss, W.; Higgins, S. J.; Leary, E.; Martin, S.; Bethell, D. The Experimental Determination of the Conductance of Single Molecules. *Phys. Chem. Chem. Phys.* **2010,** *12* (12), 2801-2815.
(50) Aragonès, A. C.; Haworth, N. L.; Darwish, N.; Ciampi, S.; Bloomfield, N. J.; Wallace, G. G.; Diez-Perez, I.; Coote, M. L. Electrostatic Catalysis of a Diels–Alder Reaction. *Nature.* **2016,** *531* (7592), 88-91.
(51) Pla-Vilanova, P.; Aragonès, A. C.; Ciampi, S.; Sanz, F.; Darwish, N.; Diez-Perez, I. The Spontaneous Formation of Single-Molecule Junctions via Terminal Alkynes. *Nanotechnol.* **2015,** *26* (38), 381001.
(52) Cowley, A.; Sze, S. Surface States and Barrier Height of Metal-Semiconductor Systems. *J. Appl. Phys.* **1965,** *36* (10), 3212-3220.
(53) Zhang, L.; Laborda, E.; Darwish, N.; Noble, B. B.; Tyrell, J. H.; Pluczyk, S.; Le Brun, A. P.; Wallace, G. G.; Gonzalez, J.; Coote, M. L. Electrochemical and Electrostatic Cleavage of Alkoxyamines. *J. Am. Chem. Soc.* **2018,** *140* (2), 766-774.
(54) Nelson, A. Co-Refinement of Multiple-Contrast Neutron/X-ray Reflectivity Data Using MOTOFIT. *J. Appl. Crystallogr.* **2006,** *39* (2), 273-276.

Graphical Abstract (TOC)